

Supplementary Information

Crystal-size effect on the kinetics of CO₂ adsorption in metal organic frameworks studied by NMR

Weiming Jiang and Kazuyuki Takeda*

Contents

1	Materials and instruments	2
1.1	Synthesis	2
1.2	Powder X-ray diffraction	2
1.3	In situ NMR	2
2	Characterizations	3
2.1	Powder XRD	3
2.2	Microscope images	5
2.3	NMR	7
3	Data fitting	9
4	Derivation of Eq. (5)	10

1 Materials and instruments

All reagents and solvents were purchased from Nacalai Tesque and used without further purification. Powder X-ray diffraction (PXRD) data were recorded on MiniFlex 400 (Rigaku) using Cu-K α radiation ($\lambda = 1.54178 \text{ \AA}$) from $2\theta = 5^\circ$ up to 40° with increment of 0.02° . Scanning electron microscopy (SEM) images of the samples were obtained using SU8000 and SU5000 (Hitachi).

1.1 Synthesis

Single crystals of $[\text{Zn}_2(1,4\text{-NDC})_2(\text{dabco})]_n\text{MOF}$ (1,4-NDC, 1,4-naphthalenedicarboxylic acid; dabco, 1,4-diaabicyclo[2.2.2]octane) were prepared according to the scheme reported by Hosono et al.¹, and washed with DMF three times. The solvent was gradually exchanged with CH_3CN for ten times in a week. The cc@CO_2 crystals were prepared by gently crushing the CH_3CN exchanged single crystals NDMOF into pieces and sieving out using 80 and 120 meshes. The pd@CO_2 crystals were prepared by stirring the solvent-exchange sample in CH_3CN at 400 rpm for two days. The spd@CO_2 crystals were prepared by stirring the solvent-exchanged sample in CH_3CN at 900 rpm for 2 days.

1.2 Powder X-ray diffraction

The crystallinity of the synthesized NDMOF was confirmed by comparing the X-ray diffraction patterns with the simulated one using the published crystalline structure of NDMOF. The crystal axes of the single crystal NDMOF were assigned by the diffraction peaks of 100 and 001 facets with different crystal alignments.

1.3 In situ NMR

The NDMOF samples were loaded in a capillaries with a diameter of 1.5 mm. The capillary was connected to a homemade gas loading setup. To remove the remaining solvent, the sample was evacuated at 160°C for 4 h. Then sample was cooled down to room temperature, and loaded with $^{13}\text{CO}_2$ at 90 kPa, and flame sealed. All ^{13}C spectra were referenced to free CO_2 gas at 125 ppm. Hahn echo experiments were used to collect static ^{13}C NMR spectra of $^{13}\text{CO}_2$ loaded NDMOF in magnetic fields of 7.05 T and 14.09 T. The exchange spectroscopy (EXSY) was performed using a standard 3 pulse sequence with 16 points in the indirect dimension with t_1 increment of 400 us. Two-dimensional (2D) data were processed by the inner product method^{2,3}. The 2D spectra in Fig. 5 were plotted with 8 contour lines corresponding to peak intensities ranging from 5% to 80%.

2 Characterizations

2.1 Powder XRD

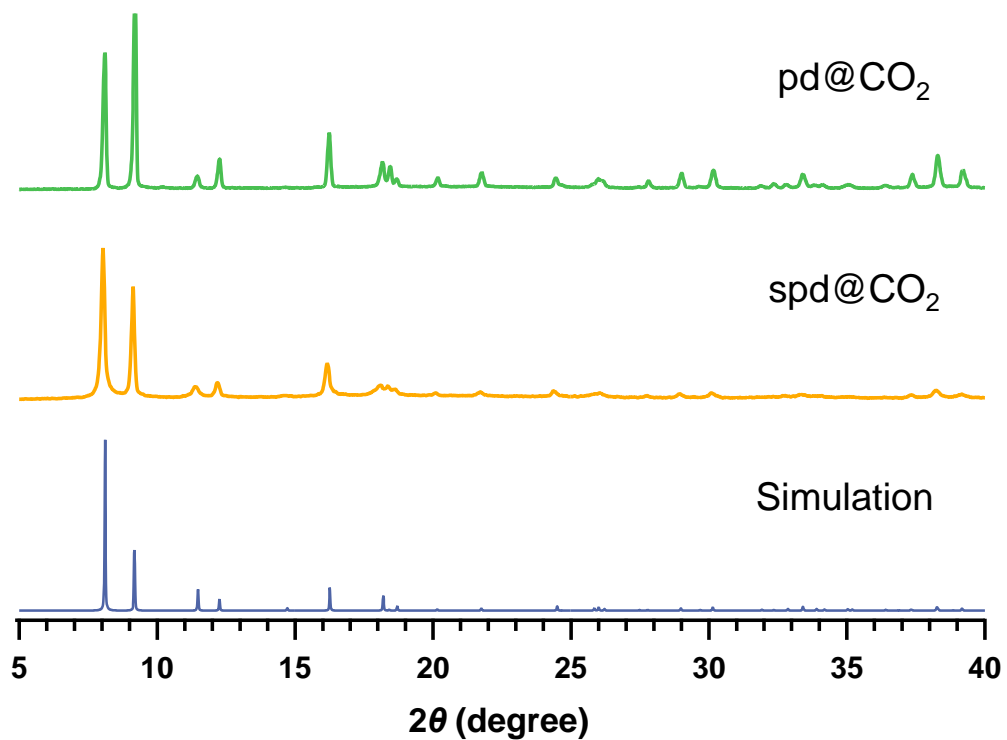


Figure S1: Measured PXRD patterns of pd@CO_2 (green line), spd@CO_2 (orange line), and a simulated powder pattern of NDMOF (blue line).

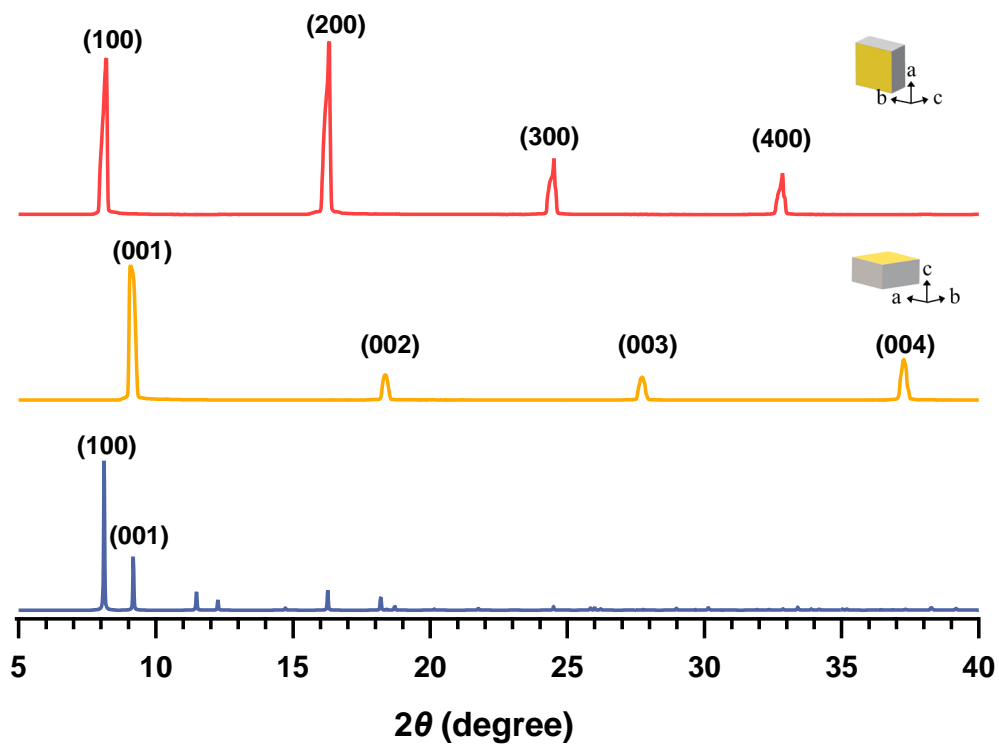


Figure S2: XRD patterns of single crystal NDMOF with two different alignments, and a simulated powder pattern of NDMOF (blue line).

2.2 Microscope images

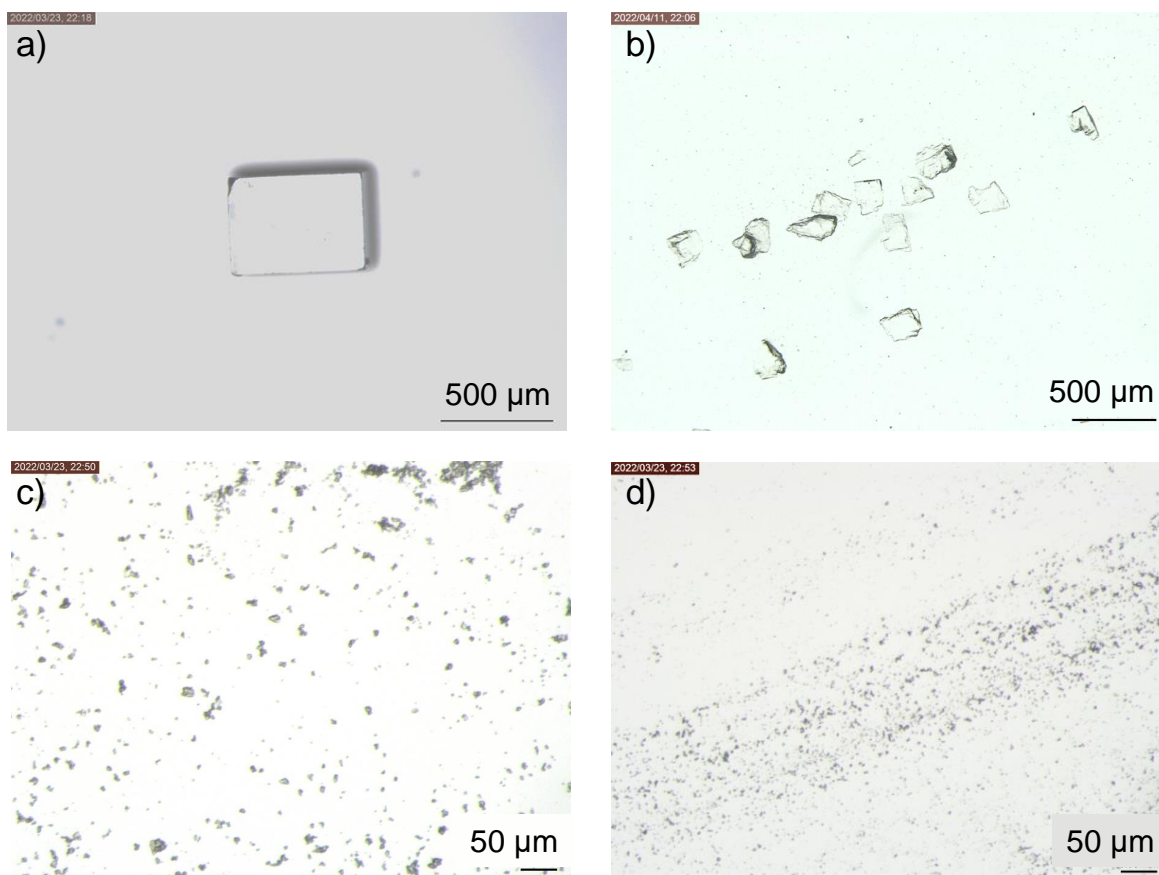


Figure S3: Optical images of the NDMOF samples. (a) a single crystal, (b) crushed crystals (denoted as cc in the text) (c) coarse powder (pd), (d) fine powder (spd).

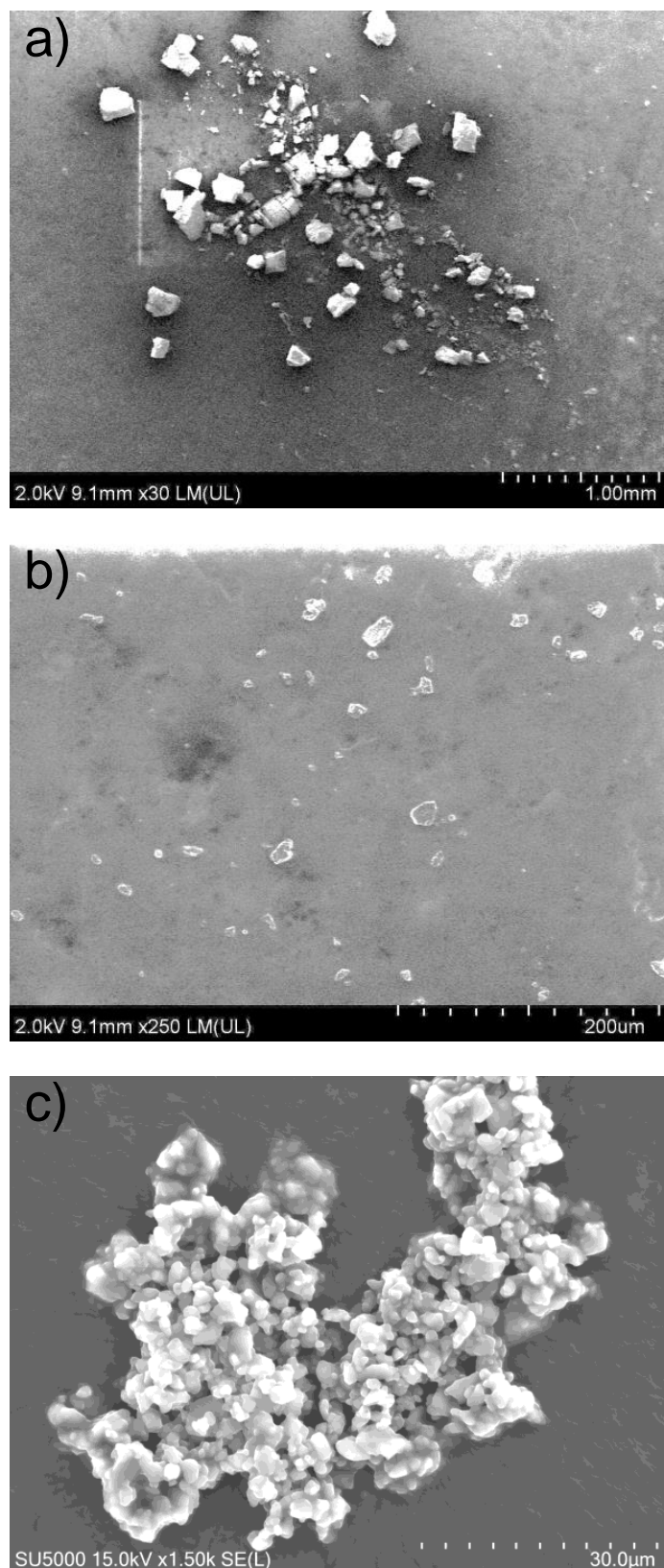


Figure S4: SEM images of the NDMOF samples. (a) crushed crystals (denoted as cc in the text) (b) coarse powder (pd), (c) fine powder (spd).

2.3 NMR

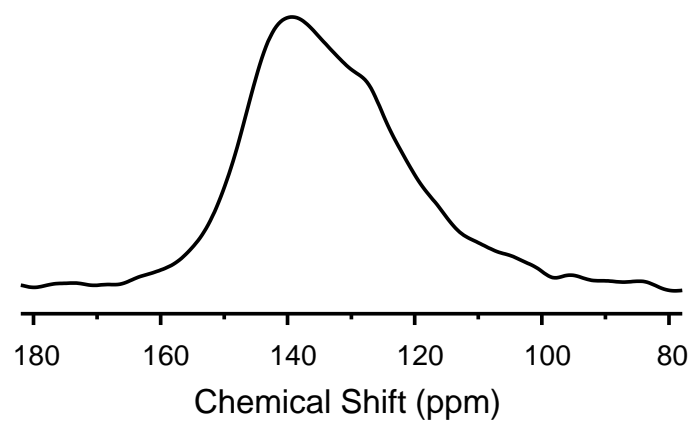


Figure S5: ^{13}C spectrum of sc@CO_2 measured at 243 K with the c -axis of the single crystal set parallel to the magnetic field B_0 .

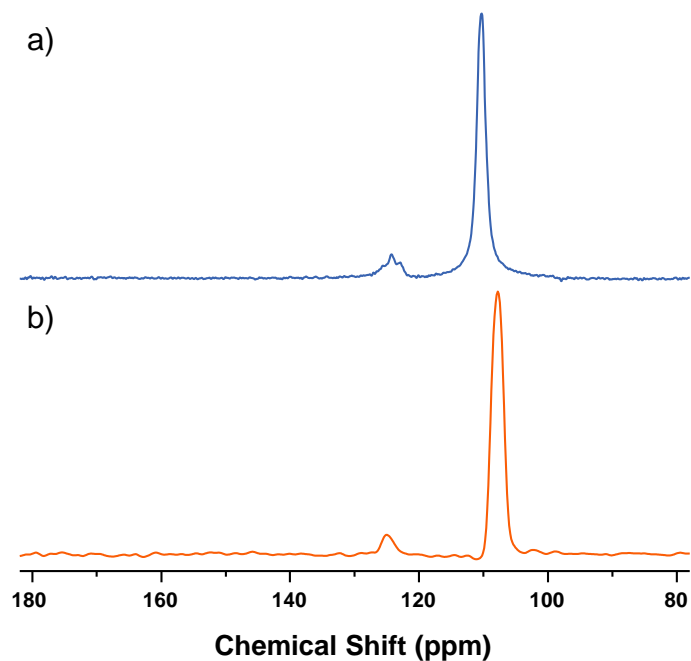


Figure S6: ^{13}C spectra of sc@CO_2 measured in magnetic fields of (a) 14.09 T and (b) 7.05 T at 303 K.

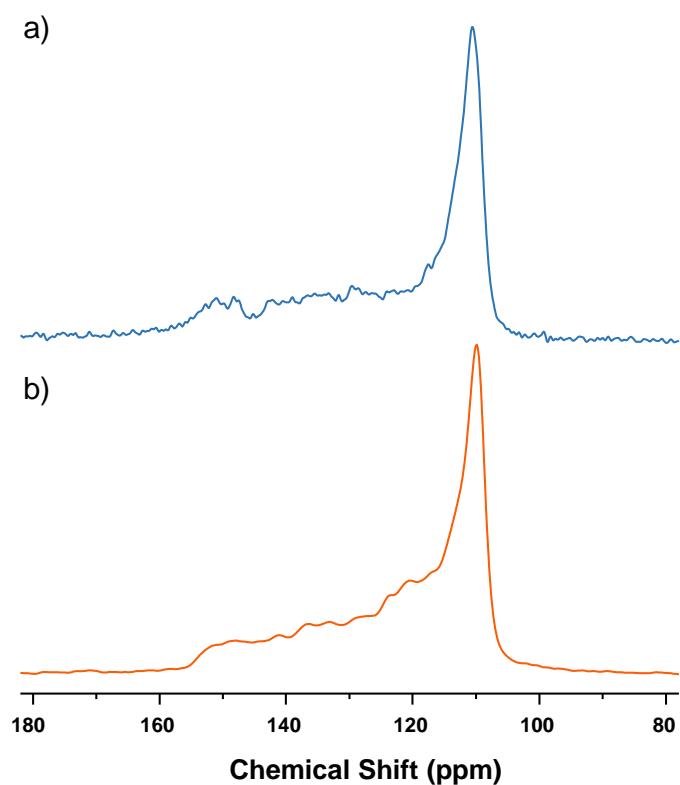


Figure S7: ^{13}C spectra of cc@CO_2 measured in magnetic fields of (a) 14.09 T and (b) 7.05 T at 303 K.

3 Data fitting

The shape $K(\omega)$ (Eq. (8)) of the ^{13}C resonance line for pd@CO₂ and cc@CO₂ was evaluated by the model described in the main text. For $I(\omega)$ (Eq. (2)), the shape of the experimental spectrum of cc@CO₂ was used. For various combinations of the kinetic parameters, $J(\omega; \omega_0\delta_{\text{iso}}, \omega_B)$ (Eq.(5)) was evaluated, and numerically integrated using discrete summation with a step of 0.05 ppm.

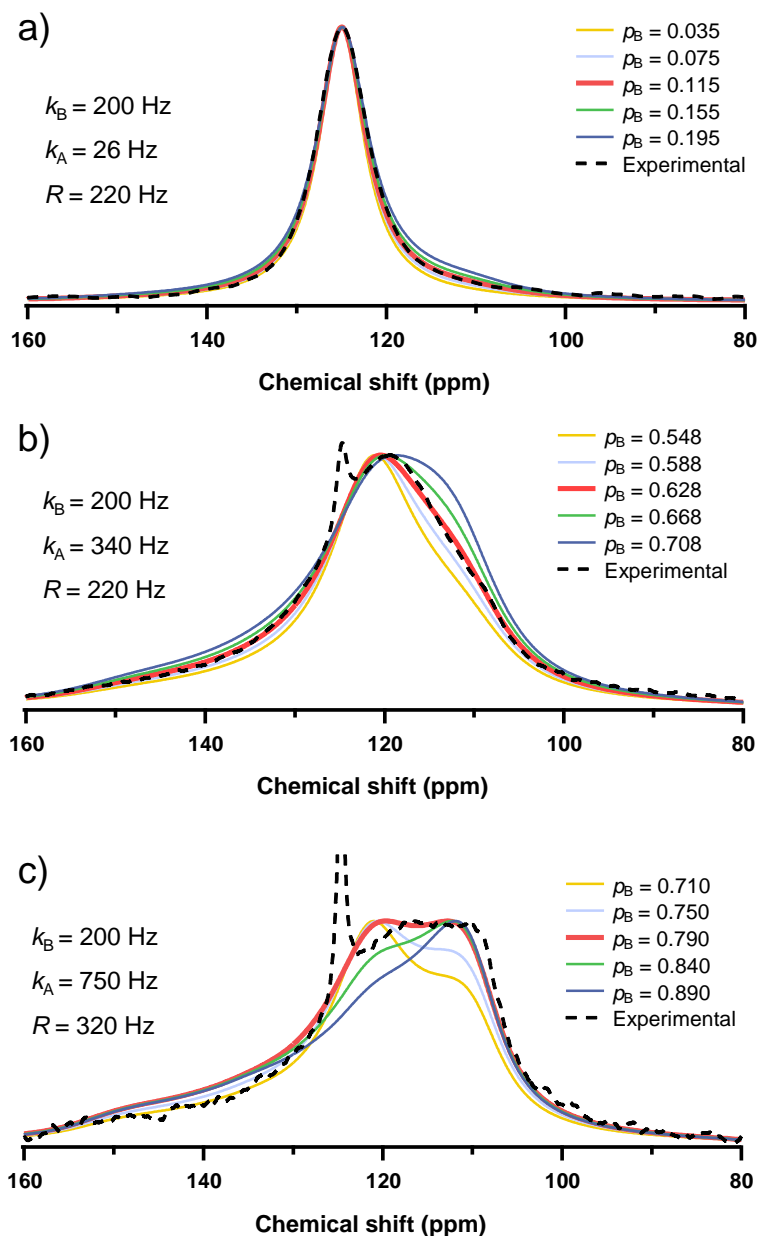


Figure S8: Comparison of the experimental spectra and the calculated spectra with varied ρ_B (a) spd@CO₂ obtained in 7.05 T, and pd@CO₂ obtained in (b) 7.05 T, (c) 14.09 T.

4 Derivation of Eq. (5)

For convenience of the readers, we show here a basic idea of how to derive Eq. (5) based on the derivation given by Římal et al.⁴

Let us consider a pair of nuclear-spin magnetizations \mathbf{M}_A and \mathbf{M}_B at asymmetrically exchanging sites A and B, respectively. The time evolution of the complex transverse components $M_A^+ = M_A^x + iM_A^y$ and $M_B^+ = M_B^x + iM_B^y$ are governed by

$$\frac{d}{dt} \begin{pmatrix} M_A^+ \\ M_B^+ \end{pmatrix} = \begin{pmatrix} -\beta_A - k_A & k_B \\ k_A & -\beta_B - k_B \end{pmatrix} \begin{pmatrix} M_A^+ \\ M_B^+ \end{pmatrix}, \quad (\text{S1})$$

where $\beta_A = R_A - i\omega_A$ and $\beta_B = R_B - i\omega_B$. To solve Eq. (S1), it is necessary to find the eigenvalues and the eigenvectors of the matrix, diagonalize it, and obtain the exponential. For details of somewhat tedious but straightforward calculation of the solution, the readers may refer to the paper by Římal et al.⁴.

Now the free induction decay (FID) as a function of time is given by $M_A^+(t) + M_B^+(t)$, and its Fourier transformation gives a complex spectrum. Its real part, Eq. (5), corresponds to the absorption spectrum for a given set of kinetic parameters k_A , k_B , and populations, p_A , p_B .

References

- [1] N. Hosono, A. Terashima, S. Kusaka, R. Matsuda and S. Kitagawa, *Nature Chemistry*, 2019, **11**, 109–116.
- [2] K. Takeda, Y. Kobayashi, Y. Noda and K. Takegoshi, *Journal of Magnetic Resonance*, 2018, **297**, 146–151.
- [3] K. Takeda, in *Annual Reports on NMR Spectroscopy*, Elsevier Ltd., 1st edn., 2020, vol. 100, pp. 153–201.
- [4] V. Římal, H. Štěpánková and J. Štěpánek, *Concepts in Magnetic Resonance Part A*, 2011, **38A**, 117–127.